Engineering Structures 56 (2013) 501–508

Contents lists available at SciVerse ScienceDirect

Engineering Structures

journal homepage: www.elsevier.com/locate/engstruct

Improvement of bridge structures to increase the safety of moving trains during earthquakes

S.H. Ju *

Department of Civil Engineering, National Cheng-Kung University, Tainan City, Taiwan, ROC

ARTICLE INFO

Article history:
Received 17 October 2012
Revised 17 May 2013
Accepted 20 May 2013
Available online 20 June 2013

Keywords:
Bridge
Derailment
Earthquake
Finite element analysis
High-speed train
Resonance

ABSTRACT

The main purpose of this study is to investigate the improvement of bridge structures to increase the safety of moving trains during earthquakes using finite element analyses, where nonlinear moving wheel elements are used to simulate the contact and separation modes of rails and wheels. The bridges are standard multi-span bridges for a high-speed rail system. The results of parametric studies with over 320 analyses indicate that the improvement in the train safety for multi-span bridges with several continuous spans is not observable. Large gaps between two simply supported girders during earthquakes will increase the train derailment coefficient, and thus a reduction in the eccentricity between two girders can enhance the safety of moving trains. Additionally, because the first train natural frequencies are often in the low frequency range, large pier stiffness producing high bridge natural frequencies can confine the train derailment coefficients near a normal value, even in the resonance between bridges and earthquakes, so we suggest that large pier stiffness should be used to ensure the safety of moving trains during earthquakes.

© 2013 Elsevier Ltd. All rights reserved.

1. Introduction

Earthquakes are a serious threat to moving high-speed trains, especially for those moving on bridges, since bridges may significantly magnify the seismic load, particularly due to the resonance that may occur among bridges, trains, and earthquakes. For example, a moderate earthquake, the Jiasian-earthquake on March 4, 2010 in southern Taiwan, derailed a high-speed train, where the maximum ground acceleration near the derailment location was only 0.17 g. Since bridges are often built for high-speed trains, avoiding train derailment on bridges is an important issue that deserves additional attention. A number of researchers used linear numerical simulations to study the dynamic behavior of moving trains attacked by earthquakes [1–6], while several researches combine theoretical and numerical methods to achieve this. Since the separation mode of the rail and wheel was not considered, the results are suitable for small or moderate seismic loads [7–11]. A few studies performed train nonlinear or derailment analyses under seismic loads. Nishimura et al. studied vehicle safety in terms of the dynamic stability and the possibility of derailment directly caused by track excitations during earthquakes, and four major outcomes for train derailment were obtained [12]. Yau presented a computational framework of interaction analysis for a maglev train traveling over a suspension bridge shaken by horizontal earthquakes, in which the suspended guideway girder was modeled as a single-span suspended beam and the maglev train traveling over it as a series of maglev masses [13]. Tanabe et al. solved the combined motion of a Shinkansen train and the railway structure during an earthquake, and a nonlinear spring element was developed to express the elastic–plastic behavior in a concrete railway structure under cyclic loads during an earthquake [14]. Ju investigated a train derailment event in southern Taiwan during the Jiasian earthquake of 2010 using the finite element method, and provided an explanation for this [15]. Du et al. presented a finite element method for the dynamic analysis of coupled bridge–train systems under non-uniform seismic ground motion, in which the rail–wheel interactions and possible separations between wheels and rails were taken into consideration [16]. Zhang et al. investigated the non-stationary random vibration of train–bridge systems subjected to multi-point earthquake excitations, and the influences of seismic apparent wave velocity and train speed on the system random responses were discussed [17]. In these various nonlinear investigations, the derailment behavior of trains can be appropriately calculated during earthquakes, but none of them focus on the improvement of bridge structures to increase the safety of moving trains.

In the structural design of bridges, it is common to select suitable member sizes to resist seismic loads, with the priority being the safety of the structure, and not the safety of moving trains. For example, engineers prefer designing a flexible structure, since less seismic loading will be generated. However, the large bridge

* Tel.: +886 6 2757575 63119; fax: +886 6 2358542.
E-mail address: juju@mail.ncku.edu.tw

0141-0296/$ - see front matter © 2013 Elsevier Ltd. All rights reserved.
http://dx.doi.org/10.1016/j.engstruct.2013.05.035

displacement due to a flexible structure may increase train derailment during earthquakes. Reducing the train speed may decrease the derailment effect [15,18], but the transportation system will be inefficient. This study will thus concentrate on investigating optimal bridge design to improve the safety of moving high-speed trains during earthquakes.

2. Train–track–bridge interaction finite element analyses

2.1. Illustration of seismic loads

The characteristics of an earthquake include its peak ground acceleration (PGA) and frequency ranges. In this study, PGA in the X and Y directions was set to 0.25 g, and in the Z direction was set to 0.08 g, where X, Y, and Z are axes in the railway, horizontal, and vertical (negative gravity) directions, respectively. Eight period ranges varied with the period spectrum T_0 (T_0 = 0.1, 0.2, 0.3, 0.5, 0.7, 1, 1.4, and 1.8 s) were used, as shown in Fig. 1a, to generate eight seismic loads in the numerical analyses, and Fig. 1b shows the acceleration for T_0 equal to 1 s. If T_0 is large the earthquake shows a low frequency vibration, and $0.5T_0$ to T_0, as shown in Fig. 1a, represents the earthquake dominant's period. These ten response spectrums with a board range of frequency distribution are sufficient to characterize most earthquakes. The seismic accelerations were then generated with the Simqke program [19] using the response spectrum. Since the applied displacements along the mesh bottom were integrated from these accelerations, all the data was modified in order to avoid spatial variability in the seismic motion (by removing the average acceleration and velocity in the integration) [20]. For simplification, the different arriving time of waves at each pier bottom was not considered.

2.2. Finite element formulation

The high-speed train is the SKS-700 type containing 12 carriages moving in the X direction with the speed of 300 km/h. Each carriage contains two bogies, and each bogie contains two wheel sets. A 3D model and information about this train is shown in Fig. 2, which indicates that the car bodies, bogies, and wheel sets are connected by springs and dampers. The Secondary suspension system between the car body and two bogies contains 12 spring-damper systems, and the primary suspension system between a wheel and bogie contains six spring-damper systems. The properties of these springs and dampers are listed in Fig. 2. Moving wheel elements, spring-damper elements, and lumped mass were then used to simulate the train, and the accuracy study of them can be found in Ref. [21]. In this study, those elements will be briefly discussed. The moving wheel element includes a wheel node and a number of target nodes, while the current wheel position equals the initial wheel position plus the duration time multiplied by the train speed. The two target nodes between which the wheel node is located can then be found, and the three-node element stiffness for the nodal displacements (d_1, θ_1, d_2, d_3, θ_3) is:

$$\mathbf{S} = \mathbf{T}^{\mathbf{T}} \begin{bmatrix} k_r & -k_r \\ -k_r & k_r \end{bmatrix} \mathbf{T}, \quad \mathbf{T} = \begin{bmatrix} 0 & 0 & 1 & 0 & 0 \\ N_1 & N_2 & 0 & N_3 & N_4 \end{bmatrix} \tag{1}$$

where d_1, θ_1, d_3, θ_3 are the translations and rotations at target nodes 1 and 3, d_2 is the translation of the wheel node, N_i = the cubic Hermitian interpolation functions, and k_r is the stiffness between the rail and wheel. Similar to the previous study [21] using the 3D solid elements and Hermit contact elements, the stiffness calculated from the static finite element contact analysis is performed to simulate the behavior between the JIS-60 rail and SKS-700 wheel. The finite element mesh is shown in Fig. 3, where 8-node brick isoparametric elements and hermit contact elements are used. Because the contact area is small, the contact stiffness between the beam center and wheel center is little dependent on the friction force, so it was not included in the analysis. Since the wheel can move horizontally on the rail, the vertical contact stiffness can be changed due to this movement. Therefore, three horizontal eccentric distances (X_c shown in Fig. 3) of −6, 0, and 20 mm were used to generate the mesh of the wheel and rail. The results of the 3D contact analysis were shown in Fig. 3, which indicates that the vertical stiffness is not sensitive to the horizontal eccentric distance. Thus, the vertical stiffness without the horizontal eccentricity was used in this study, and this assumption can largely simplify the numerical procedure but will not cause inaccuracy of the finite element analysis. In the horizontal (Y) direction, the calculated k_r is a constant of 4.3×10^4 kN/m for the contact of JIS-60 rail and SKS-700 wheel. In the vertical (Z) direction, k_r is approximately a power function, as follows:

$$k_r = a + b f_2^c \tag{2}$$

where $a = 3 \times 10^4$ kN/m, $b = 2.5 \times 10^5$ kN/m, $c = 0.254$, f_2 is the contact force between the wheel and rail, and the unit of f_2 is kN.

The internal force vector of the wheel element including the contact force f_2 is:

$$[f_1 \ m_1 \ f_2 \ f_3 \ m_3]^T = \mathbf{S}[d_1 \ \theta_1 \ d_2 \ d_3 \ \theta_3]^T - [N_1 \ N_2 \ -1 \ N_3 \ N_4] k_r r_v(X) \tag{3}$$

where (f_1, m_1, f_2, f_3, m_3) are internal forces and moments at nodes 1, 2 and 3, and the nodal forces should exclude the terms of rail irregularities $r_v(X)$.

To analyze the numerical results only from the seismic loads, rail irregularities are not included in the finite element simulations. The value of f_2 is the contact force between the wheel and rail. If it is a compressive force (negative value), the wheel and rail

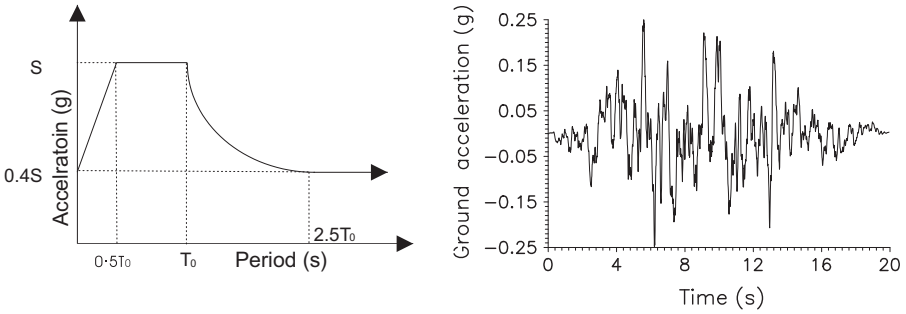

(a) Response spectrum to generate ground acceleration

(b) Ground acceleration under T_0=1 s

Fig. 1. Earthquake ground acceleration data.

Download English Version:

https://daneshyari.com/en/article/6741346

Download Persian Version:

https://daneshyari.com/article/6741346

Daneshyari.com